2014
International Symposium on Power Electronics,
Electrical Drives, Automation and Motion

Estimation of Rotor Current Based on Mathematical Model of Wound-Field Synchronous Motor Self-Excited by Space Harmonics

Masahiro Aoyama
Department of Environment and Energy System,
Graduate School of Science and Technology,
Shizuoka University and Suzuki Motor Corporation
3-5-1 Johoku, Naka-Ku, Hamamatsu,
Shizuoka 432-8561, Japan
aoyamam@hhq.suzuki.co.jp

Toshihiko Noguchi
Department of Electrical and Electronics Engineering,
Graduate School of Engineering,
Shizuoka University
3-5-1 Johoku, Naka-Ku, Hamamatsu,
Shizuoka 432-8561, Japan
ttnogut@ipc.shizuoka.ac.jp

***Abstract*— This paper describes estimation of the rotor winding current based on a mathematical model of a self-excited wound-field synchronous motor where the space harmonics power is utilized for the field magnetization instead of the permanent magnets. The operation principle of the proposed motor is explicated by a voltage equation on the synchronous rotating reference frame. Furthermore, the rotor winding current is compared between the FEM based simulation and the mathematical calculation. Consequently, it has been confirmed that both operation characteristics in the steady state agree very well and indicate similar tendency.**

Keywords—synchronous motor; self-excitation; wound field; space harmonicis; mathematical model; finite element method.

I. INTRODUCTION

Reduction of the fuel consumption and the global warming gas emission is strongly demanded from the view point of environmental conservation, and the development of such technologies is urgent matter particularly in the automotive sector [1]. Applying electric components to the power train brings a greater impact than minor improvement of conventional internal combustion engines because it is rather difficult to improve the efficiency in the low-load range with the engines [2][3]. An electric machine is one of the key components in hybrid vehicles (HEVs) and electric vehicles (EVs) from the viewpoint of the dynamic drivability and the fuel consumption performance. In general, an IPM (Interior Permanent Magnet) motor is applied to the HEV owing to its highly improved efficiency and specific power capability per physical size [4]. Permanent magnets used for the IPM motor are extremely expensive because Nd-Fe-B magnets are commonly employed to realize the high power density and to improve the fuel efficiency in the low-load operation for a street use. Moreover, the traction motors are usually installed on the chassis where special countermeasures must be taken for environmental issues. In order to mitigate demagnetization caused by the temperature rise of the permanent magnets for example, costly rare-earth metals such as Dy and Tb must be added to the Nd-Fe-B magnets.

The authors already proposed a rare-earth-free motor utilizing the space harmonics for the field magnetization power [5][6][7]. The purpose of the motor is to obtain a position of the post IPM synchronous motor by achieving the comparable torque density with the rare-earth-free configuration. The proposed motor is a kind of the self-excited wound-field synchronous motors, but is completely different from the recently proposed separate-excited wound-field machines, i.e., the wound-field flux switching motor and the brushless doubly salient motor [8][9]. The proposed motor can eliminate an external DC-coil on the primary side, which detrimentally reduces the armature coil space factor and requires an additional auxiliary chopper circuit for the excitation. In addition, it is not necessary to feed a large field current in the DC field winding for the rotor magnetization. Recently, the self-excited wound-field synchronous motor that utilizes the space harmonics for the field magnetization has been studied in the industries for the automotive traction application [10][11][12]. In the past works [10][11][[12], however, qualitative discussion on the basis of the precise mathematical model has not been accomplished to explain the operation principle of the motor because the operation characteristics have been examined only by the FEM (Finite Element Method) based electromagnetic field analysis and simple fundamental experiments. Moreover, the placement of the induction coils proposed in [10][11][12] seems not to be very efficient to retrieve the space harmonics power for the field magnetization because the single rotor winding has to play both roles of an induction coil and an electromagnet coil at the same time. On the other hand, the authors proposed the novel magnetic design that separates the induction coil from the electromagnet coil to improve the power retrieval efficiency [5]. From the authors' past investigation, the third space harmonic flux flows mainly through the rotor salient pole and the slot. This is the reason why the induction pole is placed on the *q*-axis, which is the most efficient way to retrieve the third space harmonic power.

978-1-4799-4749-2/14/$31.00 ©2014 IEEE

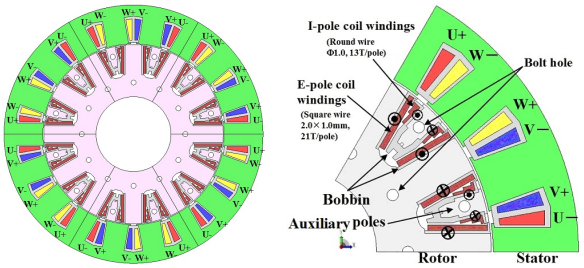

(a) Cross section diagram. (b) Detailed winding configuration.

Fig. 1. Cross section diagram of proposed motor.

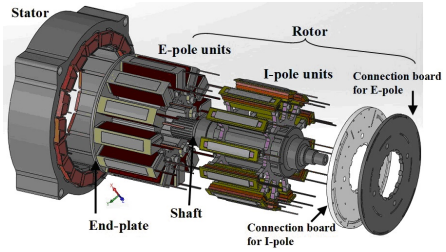

Fig. 2 Mechanical configuration of proposed motor.

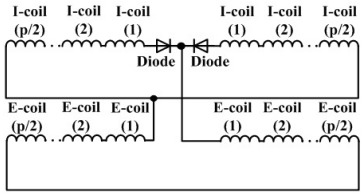

Fig. 3. Rotor winding connection of proposed motor.

TABLE I SPECIFICATION OF MOTOR.

Number of poles	12
Number of slots	18
Stator outer diameter	200 mm
Rotor diameter	138.6 mm
Axial length of core	54 mm
Air gap length	0.7 mm
Maximum current	273 A_{pk} (45s)
Stator winding resistance	32.1 mΩ / phase
Number of armature coil-turn	48
Number of I-pole coil-turn	13
Number of E-pole coil-turn	21
Winding connection	6 parallel
I-pole winding resistance	37.0 mΩ / pole
E-pole winding resistance	28.2 mΩ / pole
Thickness of iron core steel plate	0.35 mm

In this paper, the mathematical discussion of the proposed wound-field synchronous motor self-excited by the space harmonics is made. It is mathematically explained that the third space harmonics power can be mainly retrieved for the field magnetization in the discussion. The resultantly derived mathematical model allows investigating the most proper approach for the motor control. In other words, it makes possible to establish the optimum control algorithm to draw the potential abilities of the proposed motor. Moreover, the high-frequency time harmonics injection technique, which is proposed in [7][11] can be optimized while observing the rotor current condition in the low-speed range. The mathematical model of the proposed motor is discussed, followed by the simple explanation of the physical configuration of the motor. The mechanism of the field magnetization using the third space harmonics and the torque generation are investigated through the analysis. The investigated rotor current characteristics are compared with those obtained by the FEM based computer simulation, and good agreement has been confirmed between them.

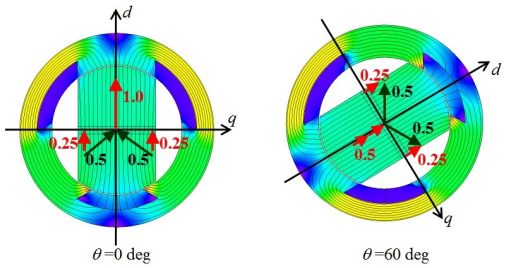

Fig. 4. *d*-axis inductance variation depending on rotor position.

II. THEORETICAL ANALYSIS OF PROPOSED MOTOR

Figure 1 shows a cross section of the proposed motor where the wound-field coils are added to the rotor salient poles, and the induction coils are placed in spaces between the rotor salient poles, i.e., the rotor slots. Each of an induction pole (I-pole) is a special pole exclusively used for the magnetizing power generation from the third space harmonics. In addition, it is magnetically independent of the main magnetic flux path to avoid the salient pole ratio degradation. I-pole is held from the axial direction using a support ring as shown in Fig. 2. On the other hand, each excitation pole (E-pole) is a salient pole on the rotor for the field excitation, which uses the retrieved third space harmonics power. All of the I-poles and the E-poles are connected in series via a diode rectifying circuit as shown in Fig. 3, where p indicates a pole number. Specifications of the motor shown in Fig. 1 are listed in TABLE I.

A. Mathematical Model on dq-Reference Frame

As shown in Fig. 4, the motor with 2-to-3-slot-combination has a *d*-axis inductance composed with a constant part and a periodical third space harmonics part according to the rotation, so the *d*-axis rotor self-inductance L_{rd} and the *q*-axis rotor self-inductance L_{rq} can be given by

$$L_{rd}(\omega t) = L_{rd0} + L_{rda}\cos 3\omega t \text{ , and} \quad (1)$$

$$L_{rq}(\omega t) = L_{rq0} + L_{rqa}\cos\left(3\omega t - \frac{\pi}{6}\right), \quad (2)$$

where L_{rd0} and L_{rq0} are the constant parts, and L_{rda} and L_{rqa} are the amplitudes of the periodical variations. ω is an electrical

synchronous angular velocity. The mathematical model of the proposed motor can be expressed as the following voltage equation:

$$\begin{bmatrix} v_{sd} \\ v_{sq} \\ v_{rd} \\ v_{rq} \end{bmatrix} = \begin{bmatrix} R_s & 0 & 0 & 0 \\ 0 & R_s & 0 & 0 \\ 0 & 0 & R_r & 0 \\ 0 & 0 & 0 & R_r \end{bmatrix} \begin{bmatrix} i_{sd} \\ i_{sq} \\ i_{rd} \\ i_{rq} \end{bmatrix} + \begin{bmatrix} \mathrm{p} & -\omega & \mathrm{p} & -\omega \\ \omega & \mathrm{p} & \omega & \mathrm{p} \\ \mathrm{p} & 0 & \mathrm{p} & 0 \\ 0 & \mathrm{p} & 0 & \mathrm{p} \end{bmatrix} \begin{bmatrix} \psi_{sd} \\ \psi_{sq} \\ \psi_{rd} \\ \psi_{rq} \end{bmatrix}$$

$$= \begin{bmatrix} R_s & 0 & 0 & 0 \\ 0 & R_s & 0 & 0 \\ 0 & 0 & R_r & 0 \\ 0 & 0 & 0 & R_r \end{bmatrix} \begin{bmatrix} i_{sd} \\ i_{sq} \\ i_{rd} \\ i_{rq} \end{bmatrix} + \begin{bmatrix} L_{sd} & 0 & M_d & 0 \\ 0 & L_{sq} & 0 & M_q \\ M_d & 0 & L_{rd} & 0 \\ 0 & M_q & 0 & L_{rq} \end{bmatrix} \mathrm{p} \begin{bmatrix} i_{sd} \\ i_{sq} \\ i_{rd} \\ i_{rq} \end{bmatrix}, \quad (3)$$

$$+ \begin{bmatrix} \mathrm{p}L_{sd} & 0 & \mathrm{p}M_d & 0 \\ 0 & \mathrm{p}L_{sq} & 0 & \mathrm{p}M_q \\ \mathrm{p}M_d & 0 & \mathrm{p}L_{rd} & 0 \\ 0 & \mathrm{p}M_q & 0 & \mathrm{p}L_{rq} \end{bmatrix} \begin{bmatrix} i_{sd} \\ i_{sq} \\ i_{rd} \\ i_{rq} \end{bmatrix}$$

$$+ \omega \begin{bmatrix} 0 & -(L_{sq}+M_q) & 0 & -(M_q+L_{rq}) \\ L_{sd}+M_d & 0 & M_d+L_{rd} & 0 \\ 0 & 0 & 0 & 0 \\ 0 & 0 & 0 & 0 \end{bmatrix} \begin{bmatrix} i_{sd} \\ i_{sq} \\ i_{rd} \\ i_{rq} \end{bmatrix}$$

where v_{sd}, v_{sq}, i_{sd} and i_{sq} are the armature voltages and currents, v_{rd}, v_{rq}, i_{rd} and i_{rq} are the d-axis and q-axis rotor winding voltages and currents, R_s and R_r are the armature winding and rotor winding resistances, M_d and M_q are the d-axis and q-axis mutual inductances, p denotes a differential operator, respectively.

The U-phase self-inductance L_u can be given by

$$L_U(\theta) = L_{S0} + L_S \cos 2\theta \,, \quad (4)$$

where L_{S0} is the constant part and L_S is the amplitude of the periodical variation of the self-inductance. Applying a rotational coordinate transform to the α-axis self-inductance L_α and the β-axis self-inductance L_β on the stationary orthogonal reference frame by using a d-axis phase θ_d and a q-axis phase θ_q, the d-axis stator self-inductance L_{sd} and the q-axis stator self-inductance L_{sq} can be obtained as

$$\begin{bmatrix} L_{sd} \\ L_{sq} \end{bmatrix} = \begin{bmatrix} \cos\omega t & \sin\omega t \\ -\sin\omega t & \cos\omega t \end{bmatrix} \begin{bmatrix} \frac{3}{2} L_S \cos 2\omega t \\ \frac{3}{2} L_S \cos\left(2\omega t - \frac{\pi}{2}\right) \end{bmatrix}. \quad (5)$$

$$= \frac{3}{2} L_S \begin{bmatrix} \cos\omega t \\ \sin\omega t \end{bmatrix}$$

Since the dq-reference frame rotates synchronously at the angular frequency ω, the L_{sd} and L_{sq} is a constant part on the dq-reference frame so that pL_{sd} and pL_{sq} equal to zero. Here, it is possible to rewrite i_{rd} and i_{rq} with i_{sd} and i_{sq} because i_{rq} is induced through the mutual inductance between the stator and the rotor. It should be noted that the third space harmonics caused by the doubly salient configuration of the motor are superimposed on i_{rq} through the induction process. As expressed in Eq. (3), the first term is the armature winding resistance drop, the second term is the transformer electromotive force, the third term is the induced electromotive force which is caused by the space harmonics,

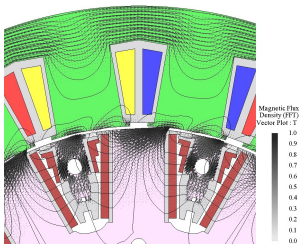

Fig. 5. Third space harmonics vector and flux lines of proposed motor.

and the forth term is the electromotive force. The induced voltage $v_{rq\text{-}ind}$ of the I-pole windings are caused by the flux linkage from the stator, which is shown in the third term in Eq. (3), so it can be expressed as

$$v_{rq-ind} = -N_{rq} \mathrm{p}\left(M_q i_{sq}\right). \quad (6)$$

By transcribing the q-axis mutual inductance M_q in the second side conversion, M_q can be simply expressed as follows by using the number of turns of the q-axis rotor windings and the stator windings N_{rq} and N_S:

$$M_q = \frac{N_S}{N_{rq}} K_q L_{rq} \,. \quad (7)$$

By substituting the above expression into Eq. (6), the induced voltage $v_{rq\text{-}ind}$ of the I-pole is obtained as follows:

$$v_{rq-ind} = -N_{rq} \mathrm{p}\left(\frac{N_S}{N_{rq}} K_q L_{rq} i_{sq}\right)$$

$$= -3\omega \frac{N_S}{N_{rq}} K_q L_{rqa} i_{sq} \sin\left(3\omega t - \frac{\pi}{6}\right), \quad (8)$$

where K_d and K_q are the leakage magnetic flux coefficients. Figure 5 shows the third space harmonics vector and the flux lines of the proposed motor. It is found that the third space harmonic flux flows mainly through the rotor salient pole and the slot. Thus, the induced voltage $v_{rd\text{-}ind}$ of the E-pole windings is caused by the d-axis space harmonic flux. This is the reason why the I-pole should be placed on the q-axis, which is the most efficient way to retrieve the both of the d-axis and the q-axis space harmonic flux. Similarly, $v_{rd\text{-}ind}$ can be given by

$$v_{rd-ind} = -3\omega \frac{N_S}{N_{rd}} K_d L_{rda} i_{sd} \sin 3\omega t \,. \quad (9)$$

The induced voltage of the I-pole and E-pole windings are applied to the E-pole windings through the full-bridge rectifier as shown in Fig. 3. Thus, the DC voltage v_{rd} applied to the E-pole windings is an absolute value of $v_{rd\text{-}ind}$ and v_{rq}, and is expressed as Eq. (10), using the Fourier series:

$$v_{rd} = \left|v_{rd-ind}\right| + \left|v_{rq-ind}\right| = a_0 + \sum_{n=1}^{\infty} \left(a_n \cos n\left(\frac{2\pi}{\frac{T}{2}}\right) t + b_n \sin n\left(\frac{2\pi}{\frac{T}{2}}\right) t \right)$$

$$= a_0 + \sum_{n=1}^{\infty} \left(a_n \cos 6n\omega t + b_n \sin 6n\omega t\right)$$

$$= \frac{3\omega}{\pi} N_S \left(\frac{\sqrt{3} K_q L_{rqa} i_{sq}}{2 N_{rq}} + \frac{3 K_d L_{rda} i_{sd}}{N_{rd}} \right) + \sum_{n=1}^{\infty} \left(a_n \cos 6n\omega t + b_n \sin 6n\omega t\right)$$

(10)

where a_0, a_n and b_n are the Fourier series coefficients. Simplifying the calculation with ignoring the time function terms, the DC voltage applied to the E-pole windings is given by the first term in Eq. (10). Since the DC voltage applied to the E-pole windings is a source of the field current i_{rd}, solving the transient response of the rotor winding gives the field current as expressed by the following equation:

$$i_{rd}(t) = \frac{v_{rd(DC)}}{R_{rq}+R_{rd}}\left(1-e^{\frac{-(R_{rq}+R_{rd})}{L_{rd}}t}\right) = \frac{3\omega}{\pi}\frac{N_S}{R_{rq}+R_{rd}}\left(\frac{\sqrt{3}K_q L_{rqa} i_{sq}}{2N_{rq}}+\frac{3K_d L_{rda} i_{sd}}{N_{rd}}\right)\left(1-e^{\frac{-(R_{rd}+R_{rq})}{L_{rd}}t}\right) \quad (11)$$

The output torque of the proposed motor is obtained by the vector product between the armature current and the magnetic flux, which is described in a part of the third term of Eq. (3):

$$\begin{aligned} T &= P_p\begin{bmatrix} i_{sd} & i_{sq}\end{bmatrix}\begin{bmatrix} 0 & -(L_{sq}+M_q) & 0 & -(L_{rq}+M_q) \\ L_{sd}+M_d & 0 & L_{rd}+M_d & 0\end{bmatrix}\begin{bmatrix} i_{sd} \\ i_{sq} \\ i_{rd} \\ i_{rq}\end{bmatrix} \\ &= P_p(L_{sd}-L_{sq})i_{sd}i_{sq} \\ &\quad + P_p\{(M_d-M_q)i_{sd}i_{sq}-(L_{rq}+M_q)i_{sd}i_{rq}+(L_{rd}+M_d)i_{rd}i_{sq}\} \\ &= P_p(L_{sd}-L_{sq})i_{sd}i_{sq} \\ &\quad + P_p\left\{\frac{1}{N_S}(N_{rd}K_dL_{sd}-N_{rq}K_qL_{sq})i_{sd}i_{sq}-\left(L_{rq}+\frac{N_{rq}}{N_S}K_qL_{sq}\right)i_{sd}i_{rq}\right. \\ &\quad \left.+\left(L_{rd}+\frac{N_{rd}}{N_S}K_dL_{sd}\right)i_{rd}i_{sq}\right\} \end{aligned} \quad (12)$$

where P_p is the pole-pair number. The coefficients have values ranging from 0 to 1. As expressed in the above expression, the output torque is composed of the two terms, i.e., the reluctance torque and the electromagnet torque. Therefore, the output torque on the dq-reference frame in the steady-state can be solved by substituting Eq. (11). Since the field current generating the electromagnet torque is proportional to ω as expressed by Eq. (11), the proposed motor cannot deliver the sufficient electromagnet torque in the low-speed range.

B. Adjustment of Motor Parameter

Because the electromagnet torque includes the leakage magnetic flux coefficients as shown in Eqs. (7) and (8) as well as the winding turn ratio between the stator and the rotor, their parameter values has significant impact on the torque generation. In addition, the d-axis and q-axis rotor self-inductances L_{rd} and L_{rq} are also important to organize the self-excitation. Figure 6 shows the d-axis and q-axis rotor magnetic flux waveforms in the steady state at 1000 r/min for 273 A_{pk} under MTPA control simulated by the FEM based magnetic field analysis. The characteristics are calculated under the condition of use of a sinusoidal current source. The rotor self-inductance is determined by fitting the dq-axis rotor magnetic flux waveform with adjusting the motor parameters L_{rd0}, L_{rq0}, L_{rda}, and L_{rqa} in Eqs. (1) and (2). As shown in Fig. 6, settings L_{rd0} = 24 μH, L_{rda} = 9 μH, L_{rq0} = 3.5 μH, and L_{rqa} = 4.7 μH are the most suitable parameters to fit the mathematically calculated results to the magnetic flux waveforms simulated by the FEM. The q-axis magnetic flux has, however, some error in the waveform. The error must be caused by having ignored the superimposed sixth space harmonics of the I-pole windings as shown in Fig. 7. Then, the d-axis and q-axis stator self-inductances are determined by fitting the reluctance torque waveform with adjusting the motor parameters L_{sd} and L_{sq}. It should be noted that L_{sd} and L_{sq} are approximated as constant parts. In general, the fluxes of the concentrated winding configuration are close to the trapezoidal waveforms, which mainly include the fifth and the seventh space harmonics, however. Separation of the reluctance torque from the electromagnet torque in the FEM result is performed through the following steps:

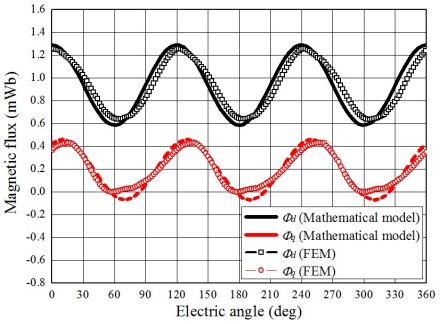

Fig. 6. dq-axes rotor magnetic flux waveform of FEM results and mathematical model results.

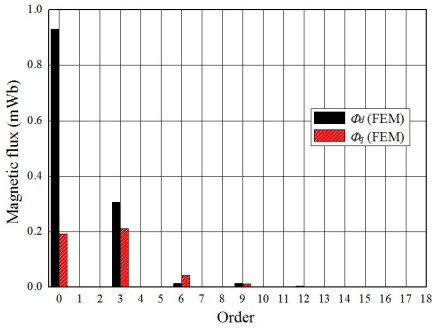

Fig. 7. Fourier series results of dq-axes rotor magnetic flux waveform of FEM results.

1) calculation of the reluctance torque at the current phase of 45 deg without connecting the rotor windings,
2) determination of the current phase vs. reluctance torque characteristic by fitting a $\sin 2\beta$ trigonometric function whose amplitude is a torque value at 45 deg calculated in the previous step,
3) calculation of the current phase vs. total torque characteristic with the rotor windings connected, and
4) subtraction of the reluctance torque from the total torque to obtain the electromagnet torque separately.

As a result, settings L_{sd} = 7.5 mH and L_{sq} = 3.5 mH are found to be the most suitable parameters under the operating condition in Fig. 6.

III. ROTOR CURRENT ESTIMATION

A. Rotor Winding Voltage

Figures 8 and 9 show the voltage of the I-pole windings v_{rq} and the E-pole windings v_{rd} of the simulated results by the FEM and the calculated results by the mathematical model in the steady state at 1000 r/min for 273 A_{pk} under MTPA control. Because the I-pole winding is connected as indicated in Fig. 2, the voltage of the I-pole windings v_{rq} is expressed as

$$\begin{aligned} v_{rq} &= v_{rq-ind} + v_{rd-ind} + (\mathrm{p}L_{rq})i_{rq} + |v_{rd}| + |v_{rq}| \\ &= v_{rq-ind} + v_{rd-ind} - 3\omega L_{rqa}\sin\left(3\omega t - \frac{\pi}{6}\right) \end{aligned} . \quad (13)$$

Similarly, the voltage of the E-pole windings v_{rd} is expressed as

$$\begin{aligned} v_{rd} &= v_{rq-ind} + v_{rd-ind} + (\mathrm{p}L_{rd})i_{rd} + |v_{rd}| + |v_{rq}| \\ &= v_{rq-ind} + v_{rd-ind} - 3\omega L_{rda}\sin(3\omega t) \end{aligned} . \quad (14)$$

The parameters adjusted in the previous section are used in Eqs. (13) and (14). As can be seen in Figs. 8 and 9, both results have overall similar characteristics with indicating the similar tendency. Particularly, some error of the waveform can be observed in the I-pole winding voltage. The error must be caused by having ignored the sixth space harmonics superposed onto the I-pole windings as shown in Fig. 6.

B. Rotor Winding Current

Figure 10 shows the rotor winding current of the I-pole i_{rq} and the E-pole i_{rd} simulated by the FEM and the mathematical model, respectively. The characteristics of the mathematical model is calculated by Eq. (11), and the I-pole winding current i_{rq} is demanded by dividing Eq. (11) by a circular constant π. It should be noted that all the I-poles and E-poles are connected in series via a diode rectifying circuit and that the armature winding is connected in parallel. Both results of the average current in the stedy state indicate very similar values. However, error is largely observed in the region where the rotor magnetization is formed in the transient state. Since the *dq*-axis magnetic flux becomes larger with respect to the rotor rotation during the time depending on the electrical rotor constant as shown in Fig. 11, the *dq*-axis rotor self-inducntace changes with respect to the rotor magnetization state.

C. Torque

Figure 12 shows the torque waveforms simulated by the FEM and the mathematical model, respectively. The leakage magnetic flux coefficients used in the mathematical model are $K_{Ld} = 0.5$ and $K_{Lq} = 0.85$, respectively. It can be confirmed that the average torque in the steady state shows good agreement, whereas the torque in the transient state does not indicate the similar behavior due to the mismatch of the rotor winding current.

IV. PRELIMINARY EXPERIMENT

It was examined by a preliminary test whether the third space harmonics link to the rotor winding and induce the voltage on the I-pole, which was theoretically discussed that the third space harmonics were caused by the double saliency

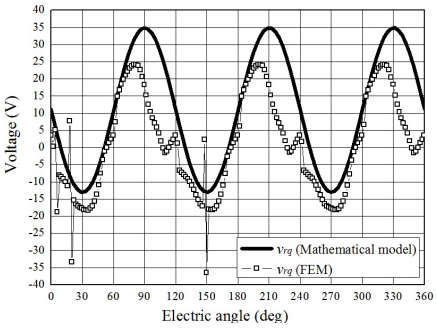

Fig. 8. I-pole winding voltage waveform of FEM result and mathematical model result.

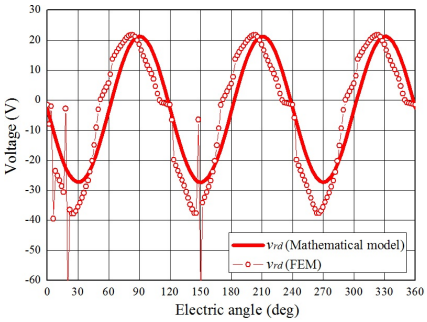

Fig. 9. E-pole winding voltage waveform of FEM result and mathematical model result.

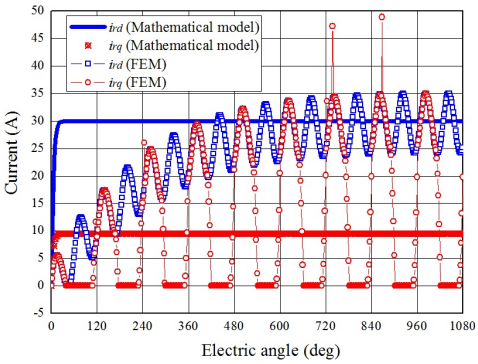

Fig. 10. *dq*-axes rotor current waveform of FEM results and mathematical model results.

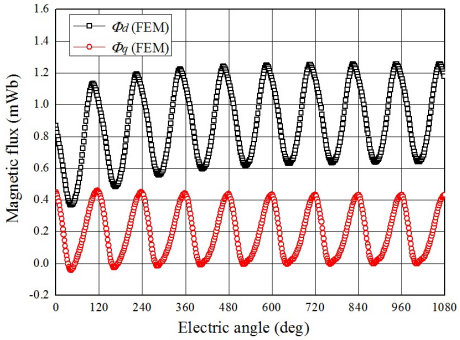

Fig. 11. *dq*-axes magnetic flux waveform of FEM results .

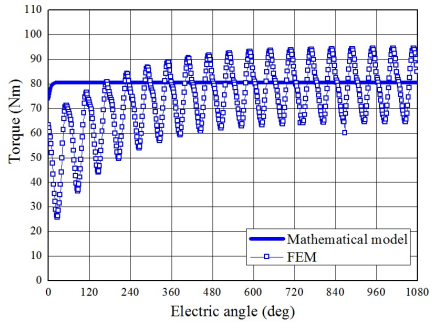

Fig. 12. Torque waveform of FEM result and mathematical model result.

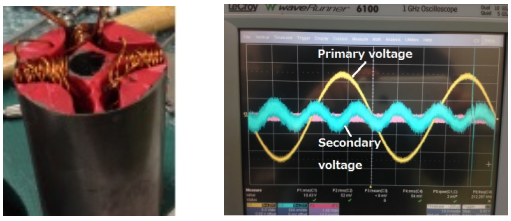

(a) SynRM with *d*-axis rotor windigs. (b) Measured voltages.

Fig. 13. Preliminary experiment by using SynRM with *d*-axis rotor windings.

and the 2-to-3-slot-combination,. As shown in Fig. 13 (a), the 4-pole 6-slot synchronous reluctance motor with additional *d*-axis rotor windings was used for the test. The sinusoidal voltages were applied to the armature windings with a linear AC power supply, and the induced voltage of the *d*-axis rotor windings was measured through a slip ring with a differential probe. As shown in Fig. 13 (b), it was confirmed that the secondary voltage, i.e., the induced voltage of the *d*-axis rotor windings had a periodical 3ω component according to the rotation.

V. CONCLUSION

This paper has presented a mathematical model of the self-excited wound-field synchronous motor where the space harmonics power is effectively utilized for the field magnetization instead of the permanent magnets. It has been clarified through the mathematical analysis and the preliminary test that the third space harmonics are the major source of the field magnetization power. In addition, the estimation of the rotor winding current based on the mathematical model have been conducted between the analyzed results by the FEM model and the calculated results by the mathematical model, which proves feasibility of the mathematical model. However, it is still necessary to brush up the mathematical model further with taking the rotor self-inductance variation into account with respect to the rotor magnetization state. The future work of the study is to develop a prototype machine and to establish a further precise mathematical model because estimation of the induced current and the field current of the rotor windings in the steady state is significantly important for the proposed

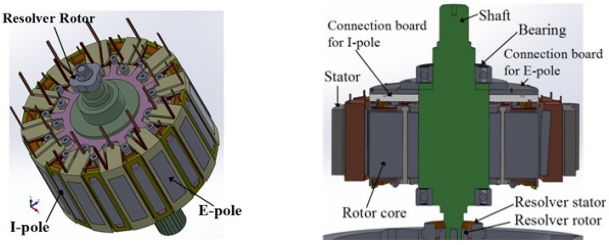

(a) Rotor assembly without rotor winding connection board. (b) Vertical cross section diagram

Fig. 14. Mechanical configuration of Prototype machine.

motor. It is also important to develop the motor parameter estimation algorithm, particularly L_{sd}, L_{sq} L_{rd}, L_{rq} and the leakage magnetic flux correction factor because mismatches of these parameters detrimentally affect the motor performance. Figure 14 illustrates the three-dimensional component exploded views of the concept prototype. Both E-pole and I-pole windings are connected with the printed circuit boards on the rotor ends as shown in Fig. 14 (b), and the diode are fixed on the boards by using resin mold.

REFERENCES

[1] Y. Sato, S. Ishikawa, T. Okubo, M. Abe, and K. Tamai, "Development of High Response Motor and Inverter System for the Nissan LEAF Electric Vehicle," *SAE Tech. Paper*, 2011-01-0350, doi: 10.4271/2011-01-0350, 2011

[2] M. Kamiya, "Development of Traction Drive Motors for the Toyota Hybrid System," *IEE-Japan Trans. on Ind. Appl.*, vol. 126, no. 4, pp.473-479, 2006.

[3] M. Okamura, E. Sato, and S. Sasaki, "Development of Hybrid Electric Drive System Using a Boost Converter," *EVS-20*, 2003.

[4] T. Fukuda and T. Eguchi, "Technology for Incresed Fuel Efficiency in New INSIGHT," *Honda R&D Tech. Rev.*, vol. 21, no. 1, 2009 (in Japanese).

[5] M. Aoyama and T. Noguchi, "Rare-Earth Free Motor with Field Poles Excited by Space Harmonics," *The 2nd ICRERA Conf. Madrid*, 978-1-4799-1464-7/13, 2013.

[6] M. Aoyama and T. Noguchi, "Mathematical Model of Novel Wound-Field Synchronous Motor Self-Excited by Space Harmonics," *The 7th IET Int. Conf. on Power Electronics, Machines and Drives*, 0071, 2014.

[7] M. Aoyama and T. Noguchi, "Preliminary Study on Active Magnetization Control of Rare-Earth Free Motor with Field Poles Excited by Space Harmonics," *IEE-Japan Tech. Meet.*, MD-13-035/RM-13-044, 2013 (in Japanese).

[8] C. Pollock, H. Pollock, R. Barron, J.R. Coles, D. Moule, A Court, and R. Sutton, "Flux-switching motors for automotive applications," *IEEE Trans. Ind. Appl.*, vol. 42, no. 5, pp. 1177-1184, 2006.

[9] L. Sun, Z. Zhang, and L. Qian, "Calculation and Analysis of Iron Loss in Doubly Salient Brushless DC Generator," *The 39th IECON Conf. Vienna*, pp. 2648-2651, 2013.

[10] K. Hiramoto and H. Nakai, "Proposal and Feasibility Study of the Integrated Diode Synchronous Motor," *IEE-Japan Ann. Meet.*, 5-054, vol. 5, pp. 97-98, 2014 (in Japanese).

[11] K. Hiramoto, H. Suzuki, H. Nakai, E. Yamada, R. Mizutani, and N. Minoshima, "Increment of the Integrated Diode Synchronous Motor in the Low Revolution Speed Area," *IEE-Japan Ann. Meet.*, 5-055, vol. 5, pp. 99-100, 2014 (in Japanese).

[12] K. Hiramoto, H. Nakai, E. Yamada, N. Minoshima, and M. Seguchi, "Rotay Electric Machine and Driving Controller for Rotary Electric Machine," *US Patent*, US20100259136 A1.